

Resonance between the Wavelength of Planar-Channeled Particles and the Period of Strained-Layer Superlattices

W. K. Chu

Department of Physics and Astronomy, University of North Carolina, Chapel Hill, North Carolina 27514

and

J. A. Ellison

Department of Mathematics, University of New Mexico, Albuquerque, New Mexico 87131

and

S. T. Picraux, R. M. Biefeld, and G. C. Osbourn

Sandia National Laboratories, Albuquerque, New Mexico 87185

(Received 11 October 1983)

A resonance effect is observed between the wavelength of a planar-channeled ion beam and the layer period of a strained-layer superlattice. Catastrophic dechanneling is observed when the wavelength and layer period are matched. A phase-rotation analysis is developed to calculate the amount of dechanneling and the amount of strain in the superlattice.

PACS numbers: 61.80.Mk, 61.50.Cj, 68.55.+b

When an ion beam enters a single crystal in a direction parallel to a set of planes, the collective atomic potential steers the ions back and forth between the planes. This oscillatory motion during channeling can be observed through the oscillations in the backscattering spectra.^{1,2} We have observed, for the first time, a resonance effect in planar dechanneling when the wavelength of the channeled-particle oscillations is matched to the period of a strained-layer superlattice (SLS). The experimental observation of this resonance effect is reported and a theoretical framework for treating planar channeling in SLS structures is developed. This work establishes the possibility of using channeled ion focusing by planes for the study of interfaces and, in this case, demonstrates the measurement of strain between layers.

Strained-layer superlattices³ are alternating layered structures with a slight lattice mismatch. During epitaxial growth, the lattice mismatch is accommodated by uniform layer strains, so that for sufficiently thin layers, no misfit defects are generated. The present studies utilized GaP/GaAs_xP_{1-x} SLS's with thirty layers of equal thickness (29 nm) of $x = 0.1$ to 0.2 grown by metal-organic chemical vapor deposition on buffer alloy layers on GaP substrates with a (100) growth orientation.

Measurements in SLS structures show good channeling along the growth direction but relatively poor channeling along inclined planar or axial

directions.^{4,5} This difference occurs because an ion beam moving along an inclined crystal plane experiences a change in planar direction, $\pm\Delta\psi$, at each interface because of the lattice strain.^{4,5} 1.2-MeV-⁴He backscattering spectra from a GaP/GaAs_xP_{1-x} sample with $x \approx 0.12$ are shown in Fig. 1 for a random direction (filled circles) and for alignment with the average {110} 45° inclined planar direction. The oscillation in the random spectrum is due to the absence of As in the second, fourth, and succeeding even layers and the energy difference between the oscillation peaks gives a thickness of 58 nm per layer pair (29 nm layer thickness). We define a superlattice

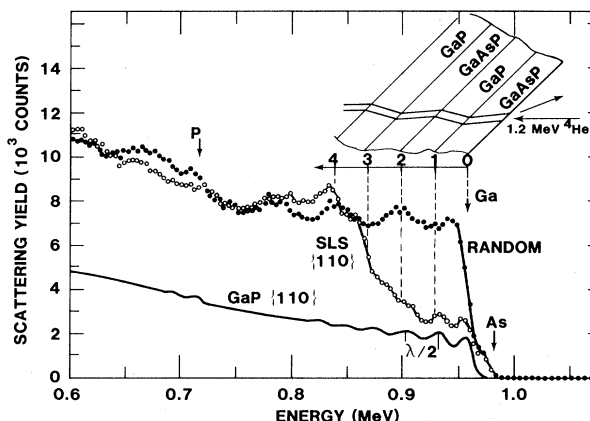


FIG. 1. Backscattering spectra for SLS and for single-crystal GaP.

period as seen by the ion beam as the distance traveled by the ions for every $\text{GaAs}_{1-x}\text{P}_x/\text{GaP}$ layer pair, which for the $\{100\}$ 45° inclined planar direction here corresponds to $58\sqrt{2} = 82$ nm. The depth scale for the Ga signal is marked in terms of the interface number, j ; thus $j = 0$ to 2 corresponds to the depth of one SLS period.

The $\{110\}$ inclined planar channeling spectrum is also given for a (100) bulk GaP crystal in Fig. 1. The oscillation in the $\{110\}$ GaP spectrum near the surface region is due to the periodic steering mentioned earlier, with the peaks occurring at distances $i\lambda/2$, where $i = 1, 2, \dots$. The channeled-particle wavelength in GaP and in the SLS sample of this composition will be almost identical. Thus from Fig. 1 the wavelength, λ , is equal to one period in this SLS for 1.2-MeV ^4He . We show below that this matching of the planar channeling wavelength to the SLS period produces an unusually high dechanneling, which is seen to occur in the SLS spectrum in Fig. 1 just below the second and third interfaces. By the depth of the fourth interface the beam has been completely dechanneled and the aligned yield exceeds that for the random direction.

The amount of $\{110\}$ planar dechanneling averaged over the top three layers as a function of energy between 0.6 to 2.0 MeV is shown in Fig. 2, with curve *a* for the SLS sample, χ_{SLS} , and curve *b* for the virgin GaP control sample, χ_v . The control sample provides the energy depen-

dence of the intrinsic dechanneling due to multiple scattering by electrons and vibrating lattice atoms. The contribution to the SLS dechanneling due to the angular shift at the interfaces, χ_s , is determined by

$$(1 - \chi_{\text{SLS}}) = (1 - \chi_s)(1 - \chi_v), \quad (1)$$

and this equation is based on the assumption of independent dechanneling mechanisms which leads to a channeling probability given by the product of the probabilities for avoiding each of the two processes. χ_s is plotted as curve *c* in Fig. 2. The peak position for curve *c* is ≈ 1.2 MeV, where the ion-beam wavelength in $\{110\}$ GaP (82 nm) matches the effective period of the SLS. We will now treat this resonance effect analytically.

Consider the ion beam to be aligned with inclined $\{110\}$ planes of a superlattice. A major portion of the beam will be channeled in the first layer, and at the first interface each particle will experience an instantaneous change in angle with respect to the new planes. The particles then continue through the second layer, however with a newly acquired transverse energy due to the tilt angle, $\Delta\psi$, at the first interface. For sufficiently large $\Delta\psi$ some of the particles will have enough transverse energy so that they become dechanneled in the second layer. This effect is repeated in each layer. The equation of motion can be written

$$d^2x/dz^2 + (1/2E)U'(x) = \sum_{j=1} (-1)^j \Delta\psi \delta(z - js), \quad (2)$$

where the coordinates x and z are shown on the top of Fig. 3, E is the incident energy, $U(x)$ is a given continuum potential⁶ of the adjacent atomic planes, $\Delta\psi$ is the angular shift change at each interface, and s is the path length per layer. Notice that Eq. (2) reduces to the usual planar continuum model for $\Delta\psi = 0$ and the delta function gives an impulse of magnitude $\Delta\psi$ to dx/dz at each interface located at $z = js$ with the first impulse in the $-dx/dz$ direction. For our experimental conditions $s = 41$ nm and $\Delta\psi \approx 0.2^\circ$. In each layer the transverse energy, E_\perp , is conserved and

$$E_\perp = E(dx/dz)^2 + U(x). \quad (3)$$

Here, x lies between $-d_p/2$ and $+d_p/2$, where d_p is the spacing between two SLS $\{110\}$ atomic planes. It has a value between 1.927 Å (GaP bulk) and 1.936 Å ($\text{GaAs}_{0.12}\text{P}_{0.88}$). We define φ_M as the angle at the center of the channel for an ion which

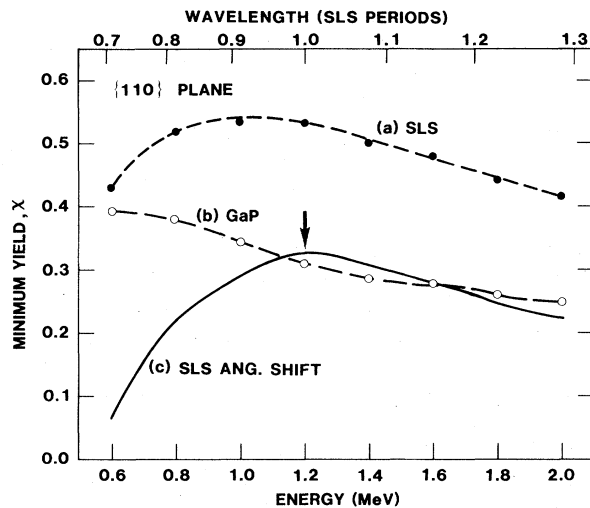


FIG. 2. Energy dependence for $\{110\}$ planar dechanneled fraction χ : curve *a*, SLS sample of Fig. 1; curve *b*, GaP single crystal; curve *c*, SLS dechanneling contribution due to the angular shifts, Eq. (1).

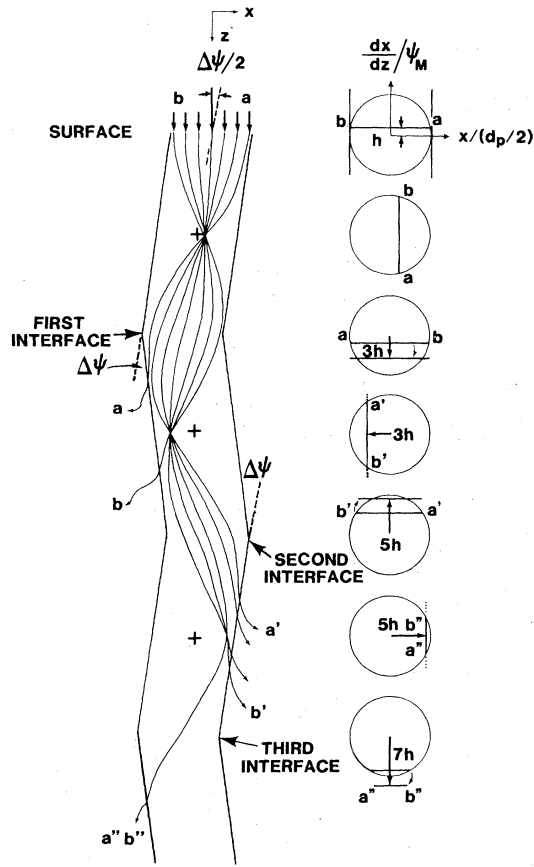


FIG. 3. Phase-plane results and schematic of corresponding planar trajectories in the SLS structure.

can just penetrate the walls²; thus

$$E\psi_M^2 = U(d_p/2). \quad (4)$$

Equation (3) can be simplified if the potential is approximated by a simple harmonic potential, $U(x) \propto x^2$, giving

$$\frac{dx^2/dz}{\psi_M^2} + \frac{x^2}{(d_p/2)^2} = r^2, \quad (5)$$

where for each particle, r is determined by its incident position and angle in each layer. Thus the motion of a particle in the phase plane is on a circle of radius r with coordinates $[2x/d_p, (dx/dz)\psi_M]$ as shown in Fig. 3. The incident ion beam is represented by the horizontal line ($a-b$) in the upper circle, and because the wavelength is independent of transverse energy in the harmonic approximation, this line rotates through an angle $\theta = 2\pi s/\lambda$ in the first layer and receives an impulse of $-\Delta\psi/\psi_M$ at the first interface. The line rotates through θ in the second layer and receives

a kick of $+\Delta\psi/\psi_M$ ($= 2h$ in Fig. 3) at the second interface. This process is repeated in succeeding layers.

This model determines the additional contribution to the dechanneling over that for a virgin crystal. The consequence of using the harmonic approximation to the continuum potential to obtain Eq. (5) is that all the particles have the same wavelength and the mixing of particle phases which occurs at deeper depths is not taken into account. However, for the first couple of periods relatively little mixing in phase occurs and this representation is valid. While a more accurate continuum potential could be used and the nonlinear problem solved numerically, considerable insight and analytic simplicity would be lost. Instead, good accuracy should be obtained in the near surface region with this model provided that the measured average wavelength λ is used and the channel-wall penetration angle ψ_M is measured or determined from more realistic potentials. Here we obtain ψ_M from Eq. (4) using a thermally averaged continuum potential obtained from the Doyle-Turner approximation to atomic potentials resulting from Hartree-Fock calculations.⁷

The result of the above model is illustrated in Fig. 3 for the catastrophic dechanneling case where the phase rotation $\theta = \pi$ per layer, corresponding to the experiment of Fig. 1. In this case the superlattice period is equal to the wavelength. Thus, in Fig. 3, a uniform parallel beam enters the surface of the crystal with a small positive incident angle $dx/dz = \Delta\psi/2$ with respect to the $\{110\}$ planes in the first layer. The particles are represented by the horizontal line in the upper circle with a normalized displacement $h = (\Delta\psi/2)/\psi_M$ from the center. As the ion beam moves down the channel, each particle undergoes a circular motion in the phase plane. At $z = s/2$ all the particles are focused at a displacement given by $h(d_p/2)$ corresponding to a phase-space rotation of $\pi/2$ (second circle). As the particles reach the first interface (third circle) the phase rotation has increased to π and they receive an impulse in the $-dx/dz$ direction by an amount $\Delta\psi$. This results in the line of particles $a-b$ being displaced $3h = (\Delta\psi + \Delta\psi/2)/\psi_M$ from the center of the circle. A portion of the beam which is outside the unit circle will be lost to dechanneling on the next 180° phase rotation as it exceeds the $x = -d_p/2$ channel wall boundary and only the portion of the beam $a'-b'$ will remain channeled. At the second interface a positive

impulse of $\Delta\psi/\psi_M$ moves $a'-b'$ from $3h$ to $5h$ and within the next layer, more than half of the beam is dechanneled as it hits the plane at $x = d_p/2$. At the third interface the downward impulse pushes all the beam outside the normalized phase circle causing the surviving portion $a''-b''$ to be totally dechanneled in the fourth layer.

One can easily see that the channeled beam location on the phase circle is progressing from h to $3h, 5h, \dots, (2j+1)h$ at the j th interface. This is equivalent to a $(2j+1)(\Delta\psi/2)$ incident angle to the plane. When $(2j+1)h \geq 1$, the beam will be focused into the channel wall in the layer(s) following the interface so that all the particles will be dechanneled. For the $(2j+1)h < 1$ case, the phase-circle description implies that the portion of the beam which will remain channeled after the j th interface is

$$(1 - \chi_j) = [1 - (2j+1)^2 h^2]^{1/2}, \quad (6)$$

where $h = \Delta\psi/2\psi_M$ and the model is valid for small j .

We have analyzed our experimental measurement (Fig. 1) of dechanneling after correction for multiple scattering [Eq. (1)] and for the initial dechanneled level in the first layer. Comparison of the results with the theoretical analysis, Fig. 3 and Eq. (6), is given in Table I. The good agreement between experiment and theory regarding the fraction of beam dechanneled after the second interface, but before the third interface, defines the value $h = 0.185$ and allows us to calculate $\Delta\psi (= 2h\psi_M)$. It is interesting to note that from the phase circle at the second interface (Fig. 3) a slight change in the value of h will make a big change in the length of $a''-b''$. Using a calculated value of $\psi_M = 0.40^\circ$ [Eq. (4)] based on the thermally averaged ($\rho_\perp = 0.067 \text{ \AA}$) continuum potential, we obtain $\Delta\psi = 0.15^\circ$. This value is somewhat smaller than, but reasonably consistent with, a value $\approx 0.2^\circ$ predicted from the elastic equations for the sample of Fig. 1 with lattice mismatch $\approx 0.4\%$.

In conclusion, we have observed a resonance effect between the wavelength of a channeled ion

TABLE I. Fraction of beam dechanneled in SLS by the angular shifts.

| No. of interfaces passed (j) | Theory ^a [Eq.(6)] | Experiment ^b (Fig. 1) |
|----------------------------------|---------------------------------|-------------------------------------|
| 0 | 0.02 | 0.00 |
| 1 | 0.17 | 0.10 |
| 2 | 0.62 | 0.62 |
| 3 | 1.00 | 1.00 |

^a χ_j for $h = 0.185$.

^b χ_s from $(1 - \chi_{\text{SLS}}) = (1 - \chi_s)(1 - \chi_v)(1 - \chi_\theta)$, where χ_{SLS} and χ_v are measured values from Fig. 1 and $\chi_\theta = 0.157$ is the dechanneled contribution due to the tilt $\Delta\psi/2$ of the first layer.

beam and the period of a strained-layer superlattice. A simple phase-rotation model is developed to calculate the dechanneling on each layer. This analysis provides a method to measure small lattice strains. It also serves to establish a basis for using planar-channeled focusing for the structural study of interface phenomena such as impurity location, interface reconstruction, and other structural effects.

This work was supported by the U. S. Department of Energy under Contract No. DE-AC04-76DP00789 and by the National Science Foundation, DMR8214301.

¹E. Bøgh, Radiat. Eff. **12**, 13 (1972); F. Abel, G. Am-sel, M. Bruneaux, and C. Cohen, Phys. Lett. **42A**, 165 (1972).

²J. H. Barrett, Phys. Rev. B **20**, 3535 (1979).

³G. C. Osbourn, R. M. Biefeld, and P. L. Gourley, Appl. Phys. Lett. **41**, 172 (1982).

⁴S. T. Picraux, L. R. Dawson, G. C. Osbourn, and W. K. Chu, to be published.

⁵W. K. Chu, J. A. Ellison, S. T. Picraux, R. M. Biefeld, and G. C. Osbourn, to be published.

⁶D. S. Gemmell, Rev. Mod. Phys. **46**, 129 (1974).

⁷P. A. Doyle and P. S. Turner, Acta Crystallogr., Sec. A **24**, 390 (1968).